

An Optimized Immunoaffinity Fluorescent Method for Natural Product Target Elucidation

Wei-luen Yu,[†] Gianni Guizzunti,[‡] Timothy L. Foley,[†] Michael D. Burkart,^{*,†} and James J. La Clair^{*,§}*Department of Chemistry and Biochemistry, University of California, San Diego, 9500 Gilman Drive, La Jolla, California 92093-0358, Department of Biology, University of California, San Diego, 9500 Gilman Drive, La Jolla, California 92093-0116, and Xenobe Research Institute, P.O. Box 4073, San Diego, California 92164-4073*

Received June 3, 2010

Understanding the mode of action of small molecules is an integral facet of drug discovery. We report an optimized immunoaffinity fluorescent method that allows one to conduct parallel studies at both the cellular and molecular level using a single probe construct. Viability of the method has been evaluated analytically and applied using glycyrrhetic acid as a model.

Understanding the networks modulated by small-molecule targets is a fundamental aspect of drug discovery.¹ Common approaches to identify natural product targets involve biomolecular extraction by tethering of the natural product to a solid-phase support, an affinity tag, a fluorescent tag, or bioorthogonal reporter.² Applications that involve a solid support are limited to molecular studies, as they are often not suitable for intracellular studies, as the binding between a natural product and its target must occur on the resin. The latter approaches develop from attachment of affinity reporters either before or after the interaction between the natural product and its target. While recent efforts expanded the methods to install reporters on small molecules, including recent examples of the Huisgen cycloaddition,³ carbene insertion chemistry,⁴ or olefin metathesis,⁵ few studies exist that compare the efficacy of these methods for identifying natural product targets.

The identification of natural product–target interactions often begins by evaluating the natural product’s activity within live cells or organisms. This often begins with the application of fluorescence microscopy to conduct a combination of uptake and localization studies. In some cases, the natural product itself delivers sufficient fluorescence, thereby obviating probe development. For the bulk of natural products, however, the attachment of a fluorescent label must address the requirements for cellular microscopy and molecular affinity, while maintaining the natural product’s native activity.⁶ In the current practice, two sets of probes are usually prepared, one for cellular imaging and the other set for affinity analyses.⁷ However, only one label and one probe are theoretically required.

Often detailed mechanistic studies on a given natural product are viewed as hit or miss operations. We are interested in providing a method that offers an analytical solution for both live cell imaging and target elucidation. Our studies began by examining a model where large quantities of the natural product were available, thereby easing the concerns with material supply for probe development. We prepared the bifunctional immunoaffinity fluorescent (IAF) probe to identify the intracellular targets of two different natural products. We seek to apply this technology to a general method for exploring the mechanism of action of bioactive compounds.

To demonstrate the method, we screened for the targets of several bioactive natural products that were available in our lab. Among them, glycyrrhetic acid (**1**) showed activity that supported its use as a model for the examining the immunoaffinity fluorescent (IAF) method. Glycyrrhetic acid (**1**) is a triterpenoid component of licorice (Figure 1), which is employed as an herbal medicine in Mediter-

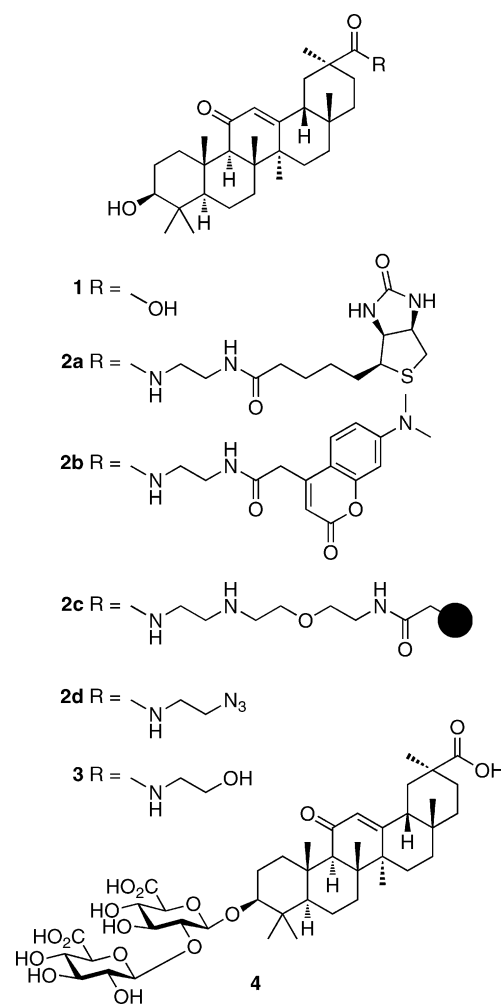


Figure 1. Structures of glycyrrhetic acid (**1**), glycyrrhetic acid probes (**2a–2d**), glycyrrhetic acid analogue **3**, and glycyrrhizic acid (**4**).

anean regions and certain areas of Asia and has been shown to display antiviral, anti-inflammatory, and antihepatocellular carcinoma activities.⁸ The active constituent of licorice extract is mainly glycyrrhizic acid (**4**), a molecule composed of two molecules of glucuronic acid and a hydrophobic fragment, glycyrrhetic acid (**1**). Actually, after oral dosing, glycyrrhizic acid (**4**) is hydrolyzed to **1** by intestinal bacteria and in the liver. In addition, affinity approaches have successfully identified protein targets (i.e., complement C3 and type IIA phospholipase A2) for glycyrrhizic acid (**4**).⁸ While

* To whom correspondence should be addressed. Tel: +001-858-401-3083. E-mail: i@xenobe.org.

[†] Department of Chemistry and Biochemistry, University of California, San Diego.

[‡] Department of Biology, University of California, San Diego.

[§] Xenobe Research Institute.

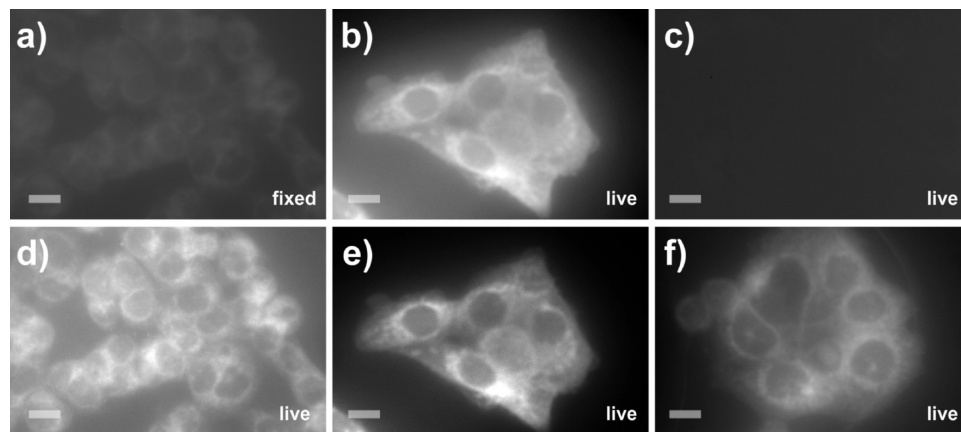


Figure 2. Uptake and subcellular localization of glycyrrhetic acid probes in HeLa cells. (a) Fluorescent image depicting HeLa cells after treatment with 10 μM probe **2a** for 6 h, washed, fixed, and then stained with 10 μM solution of blue-fluorescent IAF-tagged streptavidin. (b) HeLa cells that were treated with 10 μM probe **2b** for 6 h, washed with media and imaged live. (c) HeLa cells that were treated with a mixture of 25 μM **1** and 10 μM **2b** for 6 h, washed with media, and imaged live. Images were collected in two colors, with the blue channel depicting the probes and the red channel depicting the counterstaining with 25 μM BODIPY TR glibenclamide. (d–f) Images of the cells in (a)–(c), respectively, costained to indicate the position of the ER. Bars denote 10 μm .

series of mammalian proteins have been identified to bind to glycyrrhizic acid (**4**), understanding the human protein interactions of its metabolically released terpene **1** is far from complete. To increase the versatility for probe synthesis, terpene **1** was chosen for this study instead of glycyrrhizic acid (**4**), as its derivatization as amides such as **3** (Figure 1) was readily accomplished and shown to maintain activity.⁹ The combination of its ease in modification and established protein affinity led us to examine this natural product as a model for developing an optimized method for the elucidation of other natural product targets.

We prepared a panel of probes from glycyrrhetic acid (**1**). The panel included preparation of the biotin conjugate **2a**, immunoaffinity fluorescent probe **2b**, affinity resin **2c**, and azide terminal probe **2d**. The biotinylated probe **2a** was produced for both cellular localization and target isolation purposes. Fluorescent probe **2b** was synthesized for fluorescence microscopy, while resin-bound **2c** was well suited for target isolation studies. Probe **2d** was used for bioorthogonal reporter studies. Then we cross-evaluated each of these probes for their usage in cellular imaging and target elucidation.

HeLa cells were treated with each of the probes (Figure 2a–c) and counterstained with a panel of organelle probes (Figure 2d–f). The biotinylated probe **2a** was not suitable for live cell microscopy, as secondary staining with either a dye-labeled monoclonal antibody (mAb) against biotin or dye-labeled streptavidin was required. Moreover, even after cell fixation and secondary labeling, the fluorescence from in situ labeling of probe **2a** remained diffuse (Figure 2a). In contrast, the blue fluorescence from uptake of **2b** matched that of a red fluorescent stain for the endoplasmic reticulum (ER) (Figure 2e). Additionally, pretreatment of cells with **1** inhibited the uptake of probe **2b** (Figure 2c), indicating that **1** and **2b** were competing for the same cellular target. The combination of these observations suggested that probe **2b** localized in the ER and provides a suitable mimetic of **1**. As these studies provided clear evidence that we could develop probes for cellular imaging, we turned our attention to target elucidation.

For immunoaffinity assay, a mouse monoclonal immunoglobulin G (IgG) mAb, XRI-TF35, was generated with potent affinity to materials labeled with the 7-dimethylaminocoumarin-4-acetamide epitope (see Experimental Section) as indicated by its affinity to probe **2b** (K_d value of 0.54 ± 0.09 nM).⁶ The authors make samples of this antibody and its hybridoma accessible for open-source usage. The generation of this antibody allowed a single label in probe **2b**

to be used for fluorescence studies in living cells and protein affinity studies on cell lysate, a so-called immunoaffinity fluorescent (IAF) method.

With the XRI-TF35 mAb in hand, we examined its use to affinity purify cellular targets of **1**. Our first test was to compare the commonly used biotin–streptavidin precipitation system with the IAF tag–XRI-TF35 mAb. Bovine serum albumin (BSA) was used as a positive control to quantitatively evaluate the efficiency of protein precipitation. Samples of HeLa cell lysate were doped with BSA covalently modified with a single biotin tag (BSA-B) or IAF tag (BSA-D) (Figure 3a). The isolation of these proteins was evaluated by incubation with streptavidin–agarose or the XRI-TF35 mAb and protein A–sepharose. The retained proteins were developed on SDS-PAGE and by blot analysis (Figure 3a). Considerable background bands were observed in the biotin sample (lanes 1–4, Figure 3a) due to constitutively biotinylated proteins found in mammalian cells.¹⁰ Experiments with the IAF tag, however, returned only a single band corresponding to BSA-D (lanes 5–7, Figure 3a), with reduced background (lane 8, Figure 3a). This study indicated that the IAF/anti-IAF mAb interaction is a more selective vehicle for immunoprecipitation. It also eliminated the need to preclear lysates for background affinity partners as commonly applied in biotin–streptavidin purification methods. Quantitative analyses indicate that the limit of detection of this method was ~ 200 ng of protein by fluorescent gel imaging and ~ 2 ng of protein by western blot (Figure 3c).

As it is not always possible to label a natural product with affinity tags without affecting its activity, we evaluated the efficiency of an approach using orthogonal coupling strategies.^{3,6} The method we chose was based on the Huisgen cycloaddition between alkyne and azide groups (Figure 3e). The advantage of this approach is that the small alkyne or azide should reduce the effects that modification has on the ability of a natural product to bind to its protein target. Only after the binding has taken place in vivo is the corresponding azide or alkyne tag then coupled to the natural product probes. We evaluated the efficiency of this two-step method as compared to direct labeling (Figure 3a). Moreover, although for the cycloaddition reaction there is no difference between the combination of (a) natural product–alkyne and tag–azide or (b) natural product–azide and tag–alkyne, we additionally decided to test whether cycloadditions (a) or (b) was comparably efficient. BSA was labeled at Cys34 using the method of English with a single alkyne in **5** and azide moiety in **6**.¹¹ Azides **7** and **9** and alkynes **8** and **10** were prepared as coupling partners and used to

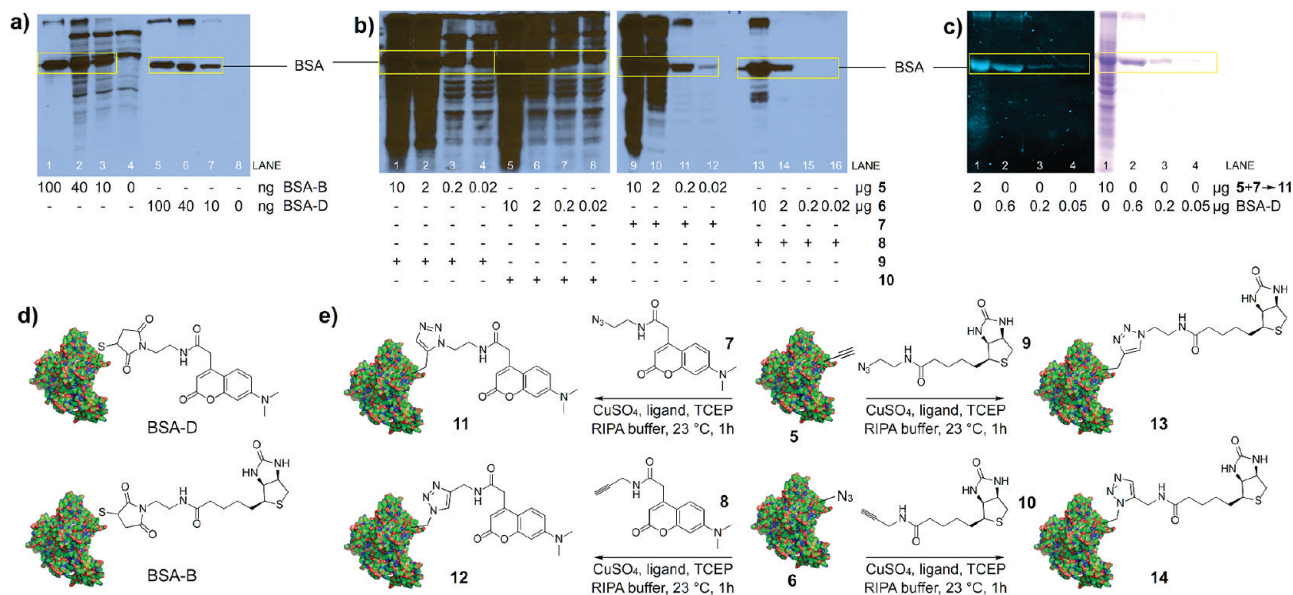


Figure 3. Protein precipitation analyses. (a) Comparison of the precipitation of biotin–streptavidin versus an anti-IAF mAb. In lanes 1–4, biotinylated BSA (BSA-B) was precipitated with streptavidin–agarose resin in the absence (lane 1) or presence (lanes 2–4) of total cell lysate. Using comparable concentrations of resin and protein, IAF-labeled BSA-D was immunoprecipitated with the XRI-TF35 mAb and protein A–sepharose (lanes 5–8). (b) Analysis of a Huisgen cycloaddition approach. BSA-alkyne **5** or BSA-azide **6** with the corresponding coupling partners **7–10** underwent copper-catalyzed cycloaddition in the presence of total cell lysate. The outcome of these reactions was given by the formation of **11–14**. The samples are then processed for SDS-PAGE and western blot. Streptavidin–HRP was used to reveal the presence of biotin (lanes 1–8). The XRI-TF35 mAb was used to detect IAF label (lanes 9–16). (c) Quantitative analysis of the Huisgen cycloaddition using both fluorescent imaging (lane 1, left) and Coomassie staining (lane 1, right) as compared to standards of BSA-D (lanes 2–4). (d) Depictions of the directly labeled BSA-D and BSA-B. (e) Huisgen cycloaddition depicting the coupling of BSA conjugates **5** and **6** to coupling partners **7–10** to form labeled proteins **11–14**. The higher molecular weight band in (a)–(c) arises from BSA aggregates. It is anticipated that a mixture of *syn*- and *anti*-triazoles is formed in **11–14**. Ligand = tris(benzyltriazolylmethyl)amine. The method is described in immunoprecipitation protocol A in the Experimental Section.

evaluate the precipitation of **11–14** from lysate (Figure 3e). This approach allowed us to compare both the choice and positioning of the reporter. Again, reactions with the biotinylated labels **9** and **10** provided background that prevented selective isolation of the labeled BSA (lanes 1–8, Figure 3b). The IAF-labeled method was more selective (lanes 9–16, Figure 3b), with optimal affinity observed between BSA-alkyne **5** and IAF-azide **7** (lanes 9–12, Figure 3b).

We then performed quantitative analyses to determine the efficiency of the two-step cycloaddition approach (Figure 3c). BSA-alkyne **5** (10 μg) was added to 200 μg of HeLa cell lysate. After cycloaddition with IAF-azide **7**, we measured the yield of adduct **11** (lane 1, Figure 3c) by comparing its fluorescence to BSA-D as a standard (lanes 2–4, Figure 3c). Using gel densitometry to measure the fluorescence intensity, we determined that the cycloaddition of **5** + **7** to **11** was quantitative (>98% yield) when run at this scale.

In isolation of cellular targets of the IAF probe, inconsistent immunoprecipitation (IP) results occurred due to different labeling methods, lysate preparations, mAb–resin conjugations, and eluting conditions. We have tested various factors and found optimal IP conditions for interpretation of results. First, the high XRI-TF35 mAb background appeared in the precipitations with hydrazide-linked Affi-Gel Hz resin and unconjugated mAb/protein A–sepharose resin (lanes 2, 3, Figure 4a). On the contrary, the amide-linked Affi-Gel 10 showed lower antibody background and was chosen as a better IP resin (lane 1, Figure 4a). Second, an unexpected nonspecific protein precipitation occurred when using probe-labeled live cell lysates in phosphate-buffered saline (PBS) buffer as the IP buffer (lanes 5, 6, Figure 4b). However, none or very few such nonspecific protein precipitations were observed with the prefrozen cell lysates in PBS buffer (lane 4, Figure 4b). To solve the nonspecific protein precipitation problem in the live cell lysate,

different cell lysis buffers were tested, and the results showed 5 mM EDTA added in the PBS buffer effectively reduced the nonspecific precipitation in the IP experiment with live cell lysates (Figure 4c). Also, the addition of a mild detergent in the lysis buffer increased the amount of protein during the lysate preparations (lane 10, Figure 4c).

With methods established, we screened for tumor cell lysates that were bound to glycyrrhetic probe **2b**. HeLa cell lysate (lane 1, Figure 5a) was immunoprecipitated with **2b** to return a protein band at 80 kDa (lane 2, Figure 5a). A sample of this band was submitted for LC-MS/MS protein ID analysis, revealing that it was protein kinase C eta (PKC η) with 56% peptide coverage. Repetition of the analysis using recombinant human PKC η (lane 3, Figure 5a) confirmed the isolation of PKC η from lysate (lane 2, Figure 5a).

Microequilibrium dialysis was conducted with recombinant PKC η to validate its affinity to **1**. These studies returned affinity measurements with K_d values of $0.64 \pm 0.12 \mu\text{M}$ to IAF probe **2b** and $0.25 \pm 0.08 \mu\text{M}$ to **1**. The identification of the binding of **2b** to a PKC is consistent with prior evidence as to the localization of PKC η in the ER,¹² the inhibition of a PKC by **1**,¹³ and the isolation of kinase targets using affinity resins bearing glycyrrhetic acid (**1a**).

We then turned to evaluate the two-step approach using glycyrrhetic azide **2d** (Figure 5b). Screening concentrations from 10 nM to 100 μM in **2d** and **8**, as well as adjusting the time and concentration of cycloaddition, failed to return PKC η . This suggested that the application of the two-step approach would require covalent attachment of **2d** to its target (PKC η) prior to cycloaddition to **8**. While analogues of **2d** could be engineered to accomplish this, the direct precipitation of PKC η by **2b** was viewed as a superior means to isolate protein targets. This suggested that two-step processes, such as the Huisgen cycloaddition, require the target protein to be covalently modified with an azide or alkyne. Recent studies further confirm this finding.¹⁴

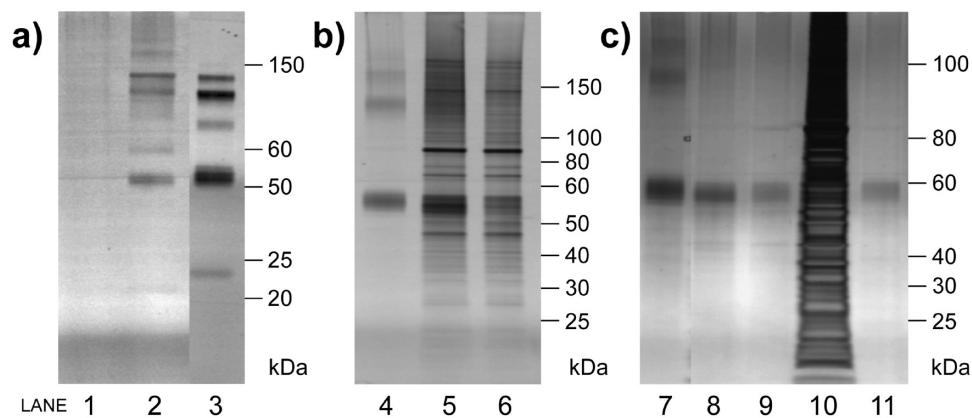


Figure 4. Further optimization of the immunoprecipitation (IP) method. (a) Blank IP test of HCT-116 cell lysate with different mAb resins: lane 1, XRI-TF35/Affi-Gel 10; lane 2, XRI-TF35/Affigel Hz; lane 3, XRI-TF35 with protein A-sepharose. (b) IP studies on frozen HCT-116 cell lysate (lane 4) and live HCT-116 cell lysate (lanes 5 and 6) in PBS buffer. IAF-labeled BSA was added to the experiments in lanes 4 and 5. Lanes 5 and 6 were fed with the IAF tag for 4 h before the lysate was prepared. (c) IP test with HCT-116 live cell lysate in different lysis buffers. IAF-labeled BSA was added to each experiment. Lanes 7-11 were eluted from reactions containing the following buffers: lane 7, PBS; lane 8, PBS with 5 mM EDTA; lane 9, PBS with 5 mM EDTA and 10 mM DTT; lanes 10, 11, PBS with 5 mM EDTA, 10 mM DTT and 1% NP-40 (lane 10, lysate before IP; lane 11, IP eluent). The method is described in immunoprecipitation protocol B in the Experimental Section.

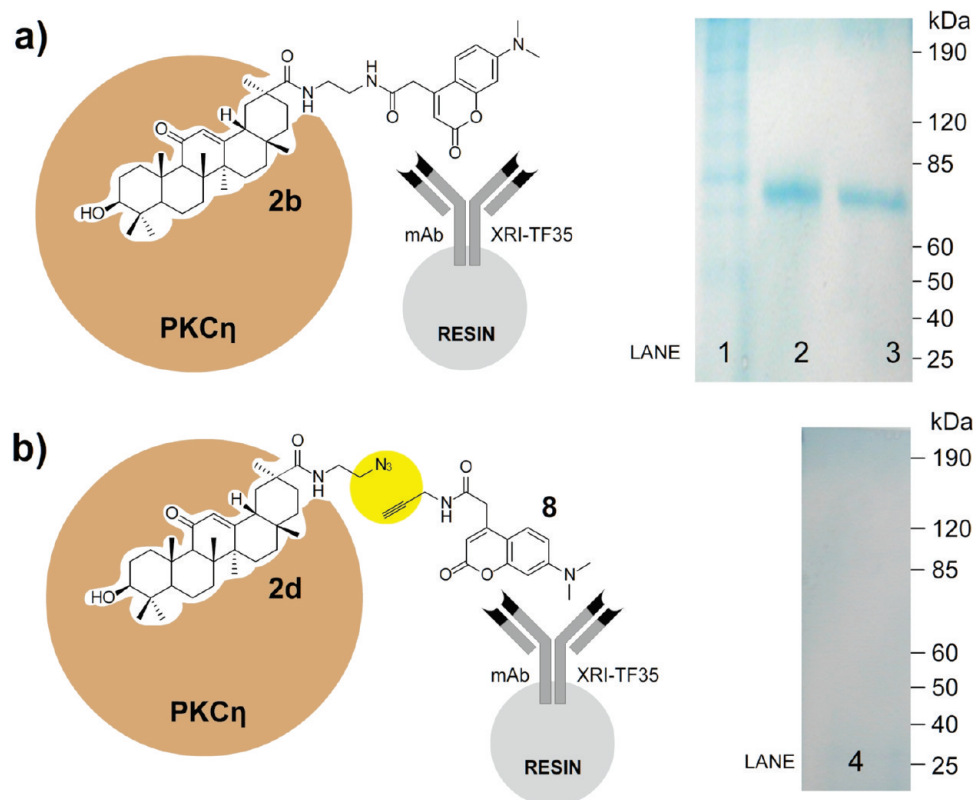


Figure 5. Elucidation of the binding of glycyrrhetic acid (**1a**) to PKC η using an IAF approach. (a) Application of the IAF-mAb precipitation method to isolate protein kinase C eta (PKC η) from HeLa cell lysates. Lane 1 of an SDS-PAGE gel depicts the total protein content of HeLa cell lysate. Lane 2 depicts the precipitated PKC η from 500 μ L of a mixture of HeLa cell lysate (1 mg mL $^{-1}$ in total protein), 100 μ M **1c**, and 100 μ L of Affi-Gel Hz resin containing the 2.5 mg mL $^{-1}$ of the XRI-TF35 mAb. Lane 3 depicts precipitation from 100 μ L of mixture containing 10 μ g mL $^{-1}$ recombinant PKC η in 1 mg mL $^{-1}$ BSA, 100 μ M **2b**, and 50 μ L Affi-Gel Hz resin containing 2.5 mg mL $^{-1}$ of the XRI-TF35 mAb. (b) Attempted two-step immunoprecipitation of PKC η by cycloaddition (shaded in yellow) of **2d** to **8**. Lane 4 of an SDS-PAGE gel depicts a lack of precipitated protein by this method.

In summary, we have shown that the combination of IAF labels and corresponding anti-IAF antibodies provides an improved system for the selective isolation of a target protein from cell lysate.¹⁵ The use of a 7-dimethylaminocoumarin-4-acetic acid label was nontoxic, provided minimal background, and did not require special pre-clearing of the lysate, a problem commonly observed when using affinity systems based on the interaction between biotin and

streptavidin.¹⁶ While other dyes and anti-dye antibodies (i.e., BODIPY dyes) may provide comparable detection, one must carefully screen each dye for potential intracellular protein affinity. The BSA standardization method (described in Figure 3) provides an effective means to control for such interactions. We have demonstrated that this is a quantitative process that can be readily controlled by comparison with standards such as BSA. We have

also optimized the immunoprecipitation condition for IAF-probe-labeled cell lysates (Figure 4). Most importantly, we demonstrated that a single probe can be used for both cellular and molecular studies. We also found that orthogonal coupling strategies can lead to a net loss in sensitivity for protein pull-down experiments when not covalently attached to their target protein.

Finally, while comparable dye and anti-dye combinations exist, the ease of probe preparation⁶ combined with the reduced nonspecific events observed during the protein affinity and cellular localization studies suggests that the 7-dimethylaminocoumarin-4-acetic acid label offers an effective vector for chemical biological studies that complement other approaches.^{16–21} As shown herein, we were able to identify protein constructs with only a two-carbon linker between the natural product and its affinity reporter. Unlike strategies that apply the combination of biotinylated natural products and streptavidin, applications using the XRI-TF35 mAb no longer require long linkages between the natural product and the reporter (i.e., typically 12–15 atoms are required for biotinylated materials)^{22–24} and therefore offer a more robust vehicle for developing probes that mimic the activity of their natural product. Additionally, the immunoprecipitation of PKC η by probe **2b** operated without a covalent linkage between the natural product probe and its protein target, thereby further expanding the repertoire of methods and applications. The methods and protocols provided herein provide a streamlined approach to rapidly screen for the targets of natural products, extending the toolbox of methods for developing a detailed understanding of the complex modes in which natural products regulate biological systems.

Experimental Section

General Experimental Procedures. NMR spectra were recorded on a Varian Mercury 400, a Varian NMR Systems 500, or a Bruker DMX500 spectrometer. Chemical shifts are reported in parts per million (ppm) on a δ scale relative to internal CDCl₃ (δ 7.26 ppm), CD₃OD (δ 3.30 ppm), or D₂O (δ 4.80 ppm) for ¹H and CDCl₃ (δ 77.00 ppm) or CD₃OD (δ 49.15 ppm) for ¹³C NMR spectra. Data for ¹H NMR are reported as follows: chemical shift, multiplicity (s = singlet, d = doublet, t = triplet, q = quartet, m = multiplet, br = broad), integration, and coupling constants. All ¹³C NMR spectra were recorded with complete proton decoupling. Spectroscopic assignments were confirmed by homonuclear COSY, gradient g-COSY, and heteronuclear gradient HSQC experiments. Low-resolution mass spectrometric analyses were performed by LCMS on an Agilent 1100 LC system coupled to an Agilent MSD/trap (ESI \pm) mass spectrometer. High-resolution mass spectrometric analyses were conducted on a ThermoFinnigan MAT900XL with reference to perfluorokerosene. Unless stated otherwise, reactions were performed in flame-dried glassware under a positive pressure of N₂ or Ar using freshly distilled solvents. Tetrahydrofuran (THF), ether, CH₂Cl₂, triethylamine, MeOH, toluene, and pyridine were freshly purified using a Seca Solvent System from Glass Contour Solvent Systems and transferred under an Ar atmosphere. Thin-layer chromatography (TLC) was accomplished using silica gel 60 F254 precoated plates (0.25 mm). Visualization of the developed chromatogram was performed by UV absorbance (254 or 365 nm), iodine on silica gel, ethanolic potassium permanganate, ethanolic 2,4-dinitrophenylhydrazine, or charring after treatment with *p*-anisaldehyde or phosphomolybdic acid. *R_f* values were obtained by elution in the stated solvent ratios (v/v). All solvent mixtures were reported as v/v unless noted otherwise. Flash chromatography and dry column vacuum chromatography were performed using silica gel (40–63 μ m particle size, 40 or 60 Å pore size and 25–40 μ m particle size, 60 Å pore size, respectively) using the indicated solvent system as eluent.

Production of the XRI-TF35 Anti-IAF mAb. A monoclonal antibody (mAb) XRI-TF35 (subclass IgG2a/ κ) directed against 7-dimethylaminocoumarin-4-acetamide (IAF label) was produced by immunizing mice with IAF-labeled keyhole limpet hemagglutinin (KLH).²⁵ KLH and bovine serum albumin were labeled with 7-dimethylaminocoumarin-4-acetic acid,⁶ providing protein that contained 0.8 and 1.2 IAF labels per protein, respectively. This was conducted by incubating 50 μ M protein in PBS pH 7.2 (137 mM NaCl, 2.7 mM KCl, 10 mM Na₂HPO₄, 1.8 mM KH₂PO₄) with five equivalents of

N-hydroxysuccinimidyl-7-dimethylaminocoumarin-4-acetate for 12 h at 4 °C. The protein was harvested by spin dialysis on a 9 kDa MWCO icon spin concentrator (Pierce) by washing with six equivalents of buffer to remove unconjugated IAF tag. Mice were immunized with 30–50 μ g of IAF-labeled KLH in RIBI MPL+TDM Emulsion Adjuvant System (Ribi Immunochem Research). Three days after the second boost (protein in PBS), spleens were dissected out, and spleen cells were mixed with the myeloma cell line Sp2/0-Ag 14 at a ratio of 4:1 and fused by using polyethylene glycol 1500.²⁵ Hybridoma screening was conducted by ELISA assay, and production of mAbs was performed according to methods previously described.²⁵ Large-scale mAb production was conducted using conventional tissue culture or by use of a Fiber Cell Bioreactor (FiberCell Systems Inc.). The XRI-TF35 cell line was cultured in mAb production medium with Advanced DMEM (Gibco 12491), 10% v/v fetal calf serum (Mediatech 35-011-CV), GlutaMAX-I Supplement (Invitrogen 35050-079), 10 mM HEPES pH 7.6 (Invitrogen), penicillin–streptomycin (Invitrogen 15070-063), Insulin–Transferrin–Selenium (ITS) growth supplement (Mediatech, 25-800-CR), and 10% v/v NCTC 109 (Gibco 21340). A typical production culture began from 10⁷ cells that were rapidly thawed from storage in liquid nitrogen and diluted with 10 mL of production medium; the cells were recovered by centrifugation at 100g. Cells were resuspended in 5 mL of media, plated in a 75 mm dish, and incubated at 37 °C in a 5% CO₂ atmosphere. At 80% confluence, cells were split 1:3 after release from the substrate by trypsinization. Cultures were expanded to ten 225 cm² and then incubated until culture media acidified, as indicated by a color change of phenol red indicator (typically 5–7 days). Culture supernatants were decanted from the flasks (a total of 850 mL), cell debris was cleared by centrifugation at 1000g, adjusted to pH 7.4 by addition of 100 mL of 10 \times PBS (1.37 M NaCl, 27 mM KCl, 100 mM Na₂HPO₄, 18 mM KH₂PO₄), and sterilized via filtration. Sterile culture supernatants were passed through two 1 mL rProtein A FF columns (Amersham Biosciences) via gravity flow at 1 mL min⁻¹. Unbound proteins were removed by washing with 25 mL of PBS and eluted with 0.1 M sodium citrate (pH 2.8) and collected in 0.8 mL fractions in tubes containing 0.2 mL of 1 M Tris base to give a final fraction pH 8.0. Protein-containing fractions were identified via Bradford assay, pooled, and buffer exchanged by repeated concentration and dilution with PBS on 9 kDa MWCO iCON spin concentrators (Pierce). XRI-TF35 mAb was concentrated to 35 mg mL⁻¹ and stored at 4 °C with thimerosal to prevent microbial growth. This protocol yielded 70 mg of purified mAb (>98% pure by SDS-PAGE).

Preparation of Mammalian Cell Lysate. HeLa cell lysate was prepared by collecting cells with a cell scraper (BD Falcon). The collected cells were diluted with lysis buffer (50 mM TrisHCl, 150 mM NaCl, 1% TX100, 0.1% SDS, protease inhibitors) and spun for 15 min at 14 000 rpm. The supernatant was collected. Proteins were concentrated using a 9 kDa MWCO iCON (Pierce) to deliver a stock solution of 1 to 5 mg mL⁻¹. All samples of HeLa cell lysate were prepared fresh, stored on ice, and used within 4 h of production. For the preparation of HCT-116 cell lysates, the PBS-washed cells from a 75 cm² culture flask were scraped and suspended in 1–2 mL of different lysis buffers with protease inhibitor cocktail (buffer contents described in Figure 4). The cell suspension was then passed through a #27.5 needle at least five times with a syringe. The crude cell lysate was filtered through a 0.45 μ m membrane to get rid of unlysed cells and nucleic acids. The frozen HCT-116 cells were stored at –80 °C for at least 16 h after the cultured cells were washed with PBS.

Uptake and Subcellular Localization in Tumor Cells. HeLa cells (ATCC CCL-2) were cultured in phenol red-free Dulbecco's modified Eagle's medium (DMEM) with 4.5 g L⁻¹ glucose, 4.5 g L⁻¹ L-glutamine, and 5% heat-inactivated fetal calf serum (FCS) in glass-bottom dishes. HCT-116 cells (ATCC CCL-247) were cultured in DMEM with 4.5 g L⁻¹ glucose, 4.5 g L⁻¹ L-glutamine, and 5% heat-inactivated FCS in glass-bottom dishes. Conventional fluorescent images were collected on a Nikon TE 2000 using irradiation with a mercury vapor lamp, filtration through a Semrock FF409 dichroic filter set with excitation at 377 \pm 50 nm, dichroic with >98% reflection at 344–404 nm and >98% transmission at 415–570 nm, and emission filter at 447 \pm 60 nm, focusing with an Zeiss Oil Immersion Epiplan 60 \times objective, and image collection with a SPOT rt-KE color CCD camera from Diagnostic Instruments. Confocal fluorescent images were collected on a Leica DMI6000 inverted confocal microscope with a Yokogawa spinning disk confocal head, Hamamatsu Orca ER high resolution B&W cooled CCD camera (6.45 μ m/pixel at 1X), Plan Apochromat 40 \times /

1.25 na and 63×/1.4 na objective, and a Melles Griot argon/krypton 100 mW air-cooled laser for 488, 568, and 647 nm excitations. Confocal z-stacks were acquired in all experiments. Costaining was conducted using either 10 μ M Syto-60 (nucleus), 25 μ M LysoTracker Red DND-99 (lysosomes), 25 μ M BODIPY TR *g*libenclamide (endoplasmic reticulum), or 25 μ M MitoTracker Red 580 (mitochondria) for 20 min, washing the cells three times with media, and collecting images in two colors (blue = probe and red = counterstain).

IAF/Anti-IAF Immunoprecipitation (Protocol A). A fixed amount of IAF-labeled bovine serum albumin BSA-D or biotinylated-bovine serum albumin BSA-B was added to a 1 mg mL⁻¹ stock of HeLa cell lysate in RIPA buffer (25 mM Tris-HCl pH 7.6, 150 mM NaCl, 1% NP-40, 1% sodium deoxycholate, and 0.1% SDS). These samples were incubated for 12 h at 4 °C with XRI-TF35 mAb and protein A resin (Figure 3a, lanes 5–8; Figure 3b, lanes 9–16) or streptavidin–agarose resin (Figure 3a, lanes 1–4; Figure 3b, lanes 1–8). Beads were collected by filtration or centrifugation at 6000 rpm and washed three times with ice-cold RIPA buffer. The beads were then collected, and gel-loading buffer (60 mM Tris pH 6.8, 5% 2-mercaptoethanol, 2% SDS, 0.01% bromophenol blue, and 10% glycerol) was added. Proteins were separated by SDS-PAGE using a 10% running gel and then transferred on a nitrocellulose membrane (western blot for 60 min at 350 mA) that was then kept in blocking buffer (50 mM Tris pH 7.5, 150 mM NaCl, 0.2% Tween 20, and 1% BSA) for 30 min. The membranes were incubated for 1 h at rt with streptavidin–HRP (BD Pharmingen) (Figure 3a, lanes 1–4; Figure 3b, lanes 1–8) or with monoclonal antibody XRI-TF35 followed by donkey anti-mouse secondary Ab–HRP (Santa Cruz) (Figure 3a, lanes 5–8; Figure 3b, lanes 9–16) diluted in blocking buffer. After washing three times (PBS, 0.2% Tween 20), the membranes were subjected to ECL (Perkin-Elmer). Kodak Biomax films were used for exposure.

IAF/Anti-IAF Immunoprecipitation (Protocol B). A sample containing 1 mg of HCT-116 lysates with or without 0.2 μ g of BSA-D in RIPA buffer was added to 50 μ L of mAb-conjugated resins or mAb-charged protein A–sepharose bead. The mixtures were incubated at 4 °C for 3 h with rotary inversion on a Thermo Scientific Labquake rotator. The resins were collected and washed three times with ice-cold wash buffer (PBS pH 7.2, 5 mM EDTA, 1% NP-40, and 0.1% SDS) and one time with PBS. The bound proteins were then eluted with 100 μ M 7-dimethylamino-4-coumarinacetic acid in PBS. The eluate proteins were analyzed by SDS-PAGE and stained with Coomassie blue or a silver staining method.

Huisgen Cycloaddition Approach. HeLa cell lysate was doped with BSA by addition of 5 μ L of a 2 mg mL⁻¹ stock BSA alkyne 4 or BSA azide 5 to 20 μ L of a 4 mg mL⁻¹ solution of HeLa cell lysate in RIPA buffer (25 mM Tris-HCl pH 7.6, 150 mM NaCl, 1% NP-40, 1% sodium deoxycholate, and 0.1% SDS). Cycloaddition reactions were conducted by sequentially adding 1 μ L of the 2.5 mM probe 6–9 in RIPA buffer containing 5% DMSO, 1 μ L of 1 mM tris(2-carboxyethyl)phosphine (TCEP), 3 μ L of a 0.1 mM solution of 0.1 mM tris(benzyltriazolylmethyl)amine, and 1 μ L of 1 mM CuSO₄ to the BSA-doped protein lysate. The mixture was diluted with the appropriate volume of buffer to make a final volume of 50 μ L and vortexed. After incubating 1–2 h at rt, 100 μ L of RIPA buffer was added to each reaction. The material was sonicated in an ultrasound bath (Branson). Proteins were precipitated from these solutions by incubating for 12 h at 4 °C with streptavidin–agarose resin (Figure 3b, lanes 1–8) or XRI-TF35 mAb and protein A resin (Figure 3b, lanes 9–16). Beads were collected by filtration or centrifugation at 6000 rpm and washed three times with ice-cold RIPA buffer. The beads were then collected, and gel loading buffer (60 mM Tris pH 6.8, 5% 2-mercaptoethanol, 2% SDS, 0.01% Bromophenol blue, and 10% glycerol) was added. Proteins were separated by SDS-PAGE using a 10% running gel and then transferred on a nitrocellulose membrane (western blot for 60 min at 350 mA) that was then kept in blocking buffer (50 mM Tris pH 7.5, 150 mM NaCl, 0.2% Tween 20, and 1% BSA) for 30 min. The membranes were incubated for 1 h at rt with streptavidin–HRP (BD Pharmingen) (Figure 3b, lanes 1–8) or with monoclonal antibody XRI-TF35 followed by donkey anti-mouse secondary Ab–HRP (Santa Cruz) (Figure 3b, lanes 9–16) diluted in blocking buffer. After washing three times (PBS, 0.2% Tween 20), the membranes were subjected to ECL (Perkin-Elmer). Kodak Biomax films were used for exposure. The amount of IAF tag incorporation was measured by comparing with BSA-D. For fluorescence analysis, the acrylamide gels were imaged by irradiation at 365 nm.

Immunoprecipitation of PKC η from HeLa Cell Lysate. A 20 μ L aliquot of 2 mg mL⁻¹ probe **2b** in DMSO solution was added to 500 μ L of HeLa cell lysate in RIPA buffer containing 1 mg mL⁻¹ in net protein. After incubation at 4 °C for 2–3 h, this solution was transferred to a second tube containing 100 μ L of Affi-Gel Hz resin (Bio-Rad) containing 2.5 mg mL⁻¹ of covalently attached XRI-TF35 mAb. The resulting mixture was shaken on a Thermo Scientific Labquake rotator for 12 h at 4 °C. The resin was then collected and washed three times with 500 μ L of ice-cold RIPA buffer. After washing was complete, five 250 μ L portions of 1 mM 7-dimethylaminocoumarin-4-acetic acid in PBS pH 7.2 were shaken vigorously with the gel for 30 min each at rt. The collected fractions were concentrated to 50 μ L on a 9 kDa MWCO icon spin concentrator (Pierce), SDS-PAGE loading buffer was added, and a 25 μ L aliquot was subjected to SDS-PAGE analysis on a NuPage 3–8% Tris-acetate gradient gel.

Immunoprecipitation of Recombinant Human PKC η . A 4.5 μ L aliquot of 2 mg mL⁻¹ probe **2b** in DMSO solution was added to 100 μ L containing 5 μ L of 1 mg mL⁻¹ recombinant human PKC η in RIPA buffer and 95 μ L of 1 mg mL⁻¹ BSA in RIPA buffer. After incubation at 4 °C for 2–3 h, this solution was transferred to a second tube containing 50 μ L of Affi-Gel Hz resin (Bio-Rad) containing 2.5 mg mL⁻¹ of covalently attached XRI-TF35 mAb. The resulting mixture was shaken on a Thermo Scientific Labquake rotator for 12 h at 4 °C. The resin was then collected and washed three times with 150 μ L of ice-cold RIPA buffer. After washing was complete, five 100 μ L portions of 1 mM 7-dimethylaminocoumarin-4-acetic acid in PBS pH 7.2 were shaken vigorously with the gel for 30 min each at rt. The collected fractions were concentrated to 30 μ L on a 9 kDa MWCO icon spin concentrator (Pierce), SDS-PAGE loading buffer was added, and a 25 μ L aliquot was subjected to SDS-PAGE analysis on a NuPage 3–8% Tris-acetate gradient gel.

Attempted Immunoprecipitation of PKC η by Huisgen Cycloaddition. A 20 μ L aliquot of 2 mg mL⁻¹ probe **2d** in DMSO solution was added to 500 μ L of HeLa cell lysate in RIPA buffer concentrated to 1 mg mL⁻¹ in net protein. After incubation at 4 °C for 2–3 h, 15 μ L of 2 mg mL⁻¹ tag **7** in DMSO, 5 μ L of 1 mM TCEP, 10 μ L of 0.1 mM tris(benzyltriazolylmethyl)amine, and 5 μ L of 1 mM CuSO₄ were added sequentially. The mixture was vortexed and then incubated for 3 h at rt. The insoluble precipitate was removed by centrifugation, and the resulting supernatant was then transferred to a second tube containing 100 μ L of Affi-Gel Hz resin (Bio-Rad) containing 2.5 mg mL⁻¹ of covalently attached XRI-TF35 mAb. The resulting mixture was shaken on a Thermo Scientific Labquake rotator for 12 h at 4 °C. The resin was then collected and washed three times with 500 μ L of ice-cold RIPA buffer. After washing was complete, five 250 μ L portions of 1 mM 7-dimethylaminocoumarin-4-acetic acid in PBS pH 7.2 were shaken vigorously with the gel for 30 min each at rt. The collected fractions were concentrated to 50 μ L on a 9 kDa MWCO icon spin concentrator (Pierce), SDS-PAGE loading buffer was added, and a 25 μ L aliquot was subjected to SDS-PAGE analysis on a NuPage 3–8% Tris-acetate gradient gel.

Protein ID Analysis. A sample of the protein in lane 2 (Figure 5a) was excised and submitted to trypsin digest LC-MS/MS analysis at the Center for Functional Genomics, University of Albany. Mass ions were searched using Mascot via GPS Explorer (version 2.0, Applied Biosystems) using the NCBIInr database. Protein identification with a confidence interval (CI%) score greater than 95% was accepted.

Microequilibrium Dialysis. Recombinant human protein kinase C η (PKC η) from *Spodoptera frugiperda* was obtained from EMD Biochemicals. Affinity constants were determined using equilibrium dialysis using a self-built PTFE Teflon 50 μ L three-well microdialysis chamber or disposable Micro DispoDIALYZER with a 25 kDa MWCO membrane (Harvard Apparatus). The association constants were determined at 23 °C in PBS pH 7.2.

***N*-(2-Azidoethyl)-2-(7-(dimethylamino)-2-oxo-2H-chromen-4-yl)acetamide (7).** 2-Azidoethylamine·HCl (61.6 mg, 0.50 mmol) was added to *N*-hydroxysuccinimidyl-7-dimethylamino-4-coumarinacetate (**15**) (86.5 mg, 0.25 mmol) with Et₃N⁺Pr (215 μ L, 1.25 mmol) in anhydrous THF (7 mL). The reaction was stirred for 12 h at rt. The contents were evaporated under reduced pressure. The desired product **7** was obtained after purification by flash chromatography (2:1 hexanes/EtOAc to 3:1 EtOAc/MeOH) as a white solid; *R*_f (0.16, 6:1 CH₂Cl₂/MeOH); ¹H NMR (500 MHz, CD₃OD, 300 K) δ 7.57 (d, *J* = 9.0 Hz, 1H), 6.75 (dd, *J* = 2.6, 9.0 Hz, 1H), 6.55 (d, *J* = 2.6 Hz, 1H), 6.05 (s, 1H), 3.70 (s, 2H),

3.40 (m, 4H), 3.07 (s, 6H); ^{13}C NMR (125 MHz, CD_3OD , 300 K) δ 170.0, 162.9, 155.8, 153.4, 151.2, 125.5, 109.2, 109.1, 108.4, 97.4, 50.1, 38.8, 38.8, 38.7; HREIMS m/z 316.1322 $[\text{M} + \text{H}]^+$ (calcd for $\text{C}_{15}\text{H}_{18}\text{N}_3\text{O}_3$ 315.1410).

2-(7-(Dimethylamino)-2-oxo-2H-chromen-4-yl)-N-(prop-2-ynyl)-acetamide (8). Propargylamine (68.6 μL , 0.40 mmol) was added to *N*-hydroxysuccinimide-7-dimethylamino-4-coumarinacetate (**15**) (69.2 mg, 0.20 mmol) with $\text{Et}_2\text{N}^i\text{Pr}$ (172 μL , 1.0 mmol) in anhydrous THF (5 mL). The reaction was stirred for 12 h at rt. The contents were evaporated under reduced pressure. The desired product alkyne **8** (52.5 mg, 92%) was obtained after purification by flash chromatography (2:1 hexanes/EtOAc to 3:1 EtOAc/MeOH) as a white solid: R_f (0.21, 3:1 $\text{CH}_2\text{Cl}_2/\text{MeOH}$); ^1H NMR (400 MHz, 3:1 $\text{CD}_3\text{OD}/\text{CDCl}_3$, 300 K) δ 7.28 (d, $J = 8.8$ Hz, 1H), 6.44 (dd, $J = 2.5, 9.0$ Hz, 1H), 6.28 (d, $J = 2.5$ Hz, 1H), 5.81 (s, 1H), 3.73 (d, $J = 2.5$ Hz, 1H), 3.43 (s, 2H), 3.11 (m, 1H), 2.82 (s, 6H), 2.09 (t, $J = 2.5$ Hz, 1H); ^{13}C NMR (100 MHz, 3:1 $\text{CD}_3\text{OD}/\text{CDCl}_3$, 300 K) 168.8, 163.2, 155.7, 153.2, 150.9, 125.8, 109.5, 109.4, 108.6, 97.9, 71.3, 39.8, 39.2, 29.0; HRESIMS m/z 285.1150 $[\text{M} + \text{H}]^+$ (calcd for $\text{C}_{16}\text{H}_{16}\text{N}_2\text{O}_3$ 284.1161).

N-(2-Azidoethyl)-5-((3aS,4S,6aR)-2-oxohexahydro-1H-thieno[3,4-d]imidazol-4-yl)pentanamide (9). 2-Azidoethylamine $\cdot\text{HCl}$ (59.0 mg, 0.48 mmol) was added to *N*-hydroxysuccinimide biotin **16** (82.2 mg, 0.24 mmol) with $\text{Et}_2\text{N}^i\text{Pr}$ (206 μL , 1.20 mmol) in anhydrous DMF (1 mL). The reaction was stirred for 12 h at rt. The contents were evaporated under reduced pressure. The desired product **9** (49.6 mg, 66%) was obtained after purification by flash chromatography (2:1 hexanes/EtOAc to 3:1 EtOAc/MeOH) as a white solid: R_f (0.15, 2:1: 0.1 $\text{CH}_2\text{Cl}_2/\text{MeOH}/\text{H}_2\text{O}$); ^1H NMR (500 MHz, CD_3OD , 300 K) δ 4.50 (dd, $J = 4.3, 7.9$ Hz, 1H), 4.31 (dd, $J = 4.5, 7.9$ Hz, 1H), 3.71 (m, 4H), 3.38 (m, 3H), 3.22 (m, 1H), 3.11 (m, 2H), 2.94 (dd, $J = 5.0, 12.7$ Hz, 1H), 2.68 (s, 1H), 2.24 (m, 1H), 1.81–1.56 (m, 3H), 1.47 (dd, $J = 7.8, 15.4$ Hz, 1H), 1.39 (d, $J = 6.6$ Hz, 1H); ^{13}C NMR (500 MHz, CD_3OD , 300 K) 175.0, 173.6, 61.9, 60.2, 55.6, 50.1, 39.6, 38.5, 35.3, 28.3, 28.1, 25.3, 24.9; HREIMS m/z 313.1367 $[\text{M} + \text{H}]^+$ (calcd for $\text{C}_{12}\text{H}_{20}\text{N}_6\text{O}_2\text{S}$ 312.1368).

5-((3aS,4S,6aR)-2-Oxohexahydro-1H-thieno[3,4-d]imidazol-4-yl)-N-(prop-2-ynyl)pentanamide (10). Propargylamine (35.2 mg, 0.29 mmol) was added to *N*-hydroxysuccinimide biotin **16** (49.1 mg, 0.14 mmol) with $\text{Et}_2\text{N}^i\text{Pr}$ (123 μL , 0.72 mmol) in anhydrous DMF (0.5 mL). The reaction was stirred for 12 h at rt. The contents were evaporated under reduced pressure. The desired product alkyne **10** (30.2 mg, 75%) was obtained after purification by flash chromatography (2:1 hexanes/EtOAc to 3:1 EtOAc/MeOH) as a white solid: R_f (0.26, 2:1:0.1 $\text{CH}_2\text{Cl}_2/\text{MeOH}/\text{H}_2\text{O}$); ^1H NMR (500 MHz, CD_3OD , 300 K) δ 4.49 (dd, $J = 4.7, 7.7$ Hz, 1H), 4.30 (dd, $J = 4.5, 7.8$ Hz, 1H), 3.94 (m, 2H), 3.21 (m, 1H), 2.93 (dd, $J = 5.0, 12.7$ Hz, 1H), 2.71 (d, $J = 12.7$ Hz, 1H), 2.63 (s, 1H), 2.57 (t, $J = 2.5$ Hz, 1H), 2.50 (t, $J = 7.2$ Hz, 1H), 2.36 (m, 1H), 2.20 (m, 2H), 1.68 (m, 4H), 1.74 (m, 2H); ^{13}C NMR (125 MHz, CD_3OD , 300 K) 174.2, 164.7, 79.2, 70.6, 61.9, 60.2, 55.5, 39.6, 35.1, 28.3, 28.0, 27.9, 25.3; HREIMS m/z 282.1196 $[\text{M} + \text{H}]^+$ (calcd for $\text{C}_{13}\text{H}_{19}\text{N}_3\text{O}_2\text{S}$ 281.1198).

(2S,4aS,6aS,6bR,10S,12aS,14bS)-10-Hydroxy-2,4a,6a,6b,9,9,12a-heptamethyl-13-oxo-N-(2-(5-((3aS,4S,6aR)-2-oxohexahydro-1H-thieno[3,4-d]imidazol-4-yl)pentanamido)ethyl)-1,2,3,4,4a,5,6,6a,6b,7,8,8a,9,10,11,12,12a,12b,13,14b-icosahydricene-2-carboxamide (2a). Biotin azide **9** (82.2 mg, 0.29 mmol) was reduced by treatment with PPh_3 (188.24 mg, 0.72 mmol) in wet THF (5 mL) for 12 h. The solvent was removed in vacuo, and the resulting wax was titrated with hexanes (3 \times 15 mL) to remove the excess triphenylphosphine. The resulting amine **17** was used further without purification. HATU (163.7 mg, 0.43 mmol) was added to a mixture of glycyrrhetic acid (**1**) (49.0 mg, 0.17 mmol), **17** (0.29 mmol, crude), and Et_3N (122 μL , 0.72 mmol) in anhydrous DMF (1.5 mL). The reaction was stirred for 16 h at rt. The contents were evaporated under reduced pressure. The desired product **2a** (82.6 mg, 78%) was obtained after purification by flash chromatography (2:1 hexanes/EtOAc to 1:1 EtOAc/MeOH) as a white solid: R_f (0.21, 3:1 $\text{CH}_2\text{Cl}_2/\text{MeOH}$); ^1H NMR (500 MHz, CD_3OD , 300 K) δ 5.69 (s, 1H), 4.51 (ddd, $J = 0.9, 5.0, 7.9$ Hz, 1H), 4.34 (dd, $J = 4.7, 7.8$ Hz, 1H), 3.35 (m, 2H), 3.31 (bs, 1H), 3.29 (m, 1H), 3.23 (m, 1H), 3.18 (m, 1H), 3.01 (s, 1H), 2.95 (dd, $J = 5.0, 12.8$ Hz, 1H), 2.88 (s, 1H), 2.85 (s, 2H), 2.73 (m, 2H), 2.58 (m, 2H), 2.45 (s, 1H), 2.01–1.36 (m, 25H), 1.43 (s, 3H), 1.15 (s, 6H), 1.13 (s, 3H), 1.01 (s, 3H), 0.84 (s, 3H), 0.81 (s, 3H); 0.77 (m, 1H); ^{13}C NMR (125 MHz, CD_3OD , 300 K) δ 202.7, 179.3, 172.6, 172.0, 170.3, 122.2, 79.2, 63.4, 63.3, 61.8, 57.0, 56.3, 46.9, 45.0, 44.7, 42.6, 41.2, 40.5, 40.4, 39.0, 38.5,

34.0, 33.1, 32.1, 31.6, 29.9, 29.4, 28.8, 28.0, 27.2, 26.6, 25.8, 24.0, 19.5, 18.8, 17.1, 16.5; HRESIMS m/z 739.4751 $[\text{M} + \text{H}]^+$ (calcd for $\text{C}_{42}\text{H}_{66}\text{N}_4\text{O}_5\text{S}$, 738.4754).

(2S,4aS,6aS,6bR,10S,12aS,14bS)-N-(2-(7-(Dimethylamino)-2-oxo-2H-chromen-4-yl)acetamido)ethyl)-10-hydroxy-2,4a,6a,6b,9,9,12a-heptamethyl-13-oxo-1,2,3,4,4a,5,6,6a,6b,7,8,8a,9,10,11,12,12a,12b,13,14b-icosahydricene-2-carboxamide (2b). HATU (189.7 mg, 0.50 mmol) was added to a mixture of glycyrrhetic acid (**1**) (78.3 mg, 0.17 mmol) and 2-aminoethyl-7-dimethylamino-4-coumarinacetamide (**18**)⁶ (134.2 mg, 0.33 mmol) or made by reduction of **7** and Et_3N (142 μL , 0.83 mmol) in anhydrous DMF (1.2 mL). The reaction was stirred for 17 h at rt. The contents were evaporated under reduced pressure. The desired product **2b** (92.1 mg, 75%) was obtained after purification by flash chromatography (2:1 hexanes/EtOAc to 3:1 EtOAc/MeOH) as a white solid: R_f (0.16, 4:1 $\text{CH}_2\text{Cl}_2/\text{MeOH}$); ^1H NMR (500 MHz, CD_3OD , 300 K) δ 7.57 (dd, $J = 0.8, 9.0$ Hz, 1H), 6.75 (dd, $J = 2.6, 9.0$ Hz, 1H), 6.56 (d, $J = 2.5$ Hz, 1H), 6.11 (s, 1H), 5.56 (s, 1H), 3.67 (m, 4H), 3.45 (m, 1H), 3.39–3.31 (m, 2H), 3.27 (m, 2H), 3.18 (m, 2H), 3.07 (s, 6H), 2.84 (s, 1H), 2.81 (s, 2H), 2.72 (dt, $J = 3.4, 13.2$ Hz, 1H), 2.45 (s, 1H), 2.13 (m, 2H), 1.91 (s, 3H), 1.83–1.12 (m, 11H), 1.43 (s, 3H), 1.13 (s, 3H), 1.03 (s, 3H), 1.00 (s, 3H), 0.80 (s, 3H), 0.79 (s, 3H); ^{13}C NMR (125 MHz, CD_3OD , 300 K) δ 202.7, 179.4, 172.7, 172.1, 164.4, 157.2, 155.0, 129.3, 129.1, 128.9, 128.7, 110.8, 110.1, 104.2, 99.0, 79.2, 63.3, 56.3, 46.8, 44.8, 44.7, 42.6, 40.4, 38.9, 38.5, 34.0, 33.0, 29.7, 29.3, 28.8, 28.0, 27.7, 27.6, 23.9, 19.4, 18.8, 18.6, 17.1, 16.5; HRESIMS m/z 742.4718 $[\text{M} + \text{H}]^+$ (calcd for $\text{C}_{45}\text{H}_{63}\text{N}_3\text{O}_6$, 741.4711).

(2S,4aS,6aS,6bR,10S,12aS,14bS)-3H-[1,2,3]Triazololo[4,5-*b*]pyridin-3-yl-10-hydroxy-2,4a,6a,6b,9,9,12a-heptamethyl-13-oxo-1,2,3,4,4a,5,6,6a,6b,7,8,8a,9,10,11,12,12a,12b,13,14b-icosahydricene-2-carboxylate (19). HBTU (148.9 mg, 0.39 mmol) was added to a mixture of glycyrrhetic acid (**1**) (92.2 mg, 0.20 mmol) and Et_3N (167 μL , 0.98 mmol) in anhydrous DMF (2 mL). The reaction was stirred for 6 h at rt. The contents were evaporated under reduced pressure. Compound **19** (89.2 mg, 77%) was obtained after purification by flash chromatography (4:1 hexanes/EtOAc to EtOAc) as a white solid: R_f (0.45, 2:1 hexanes/EtOAc); ^1H NMR (400 MHz, CDCl_3 , 300 K) δ 8.70 (dd, $J = 1.2, 4.5$ Hz, 1H), 8.38 (dd, $J = 1.2, 8.4$ Hz, 1H), 7.40 (dd, $J = 4.5, 8.4$ Hz, 1H), 5.78 (s, 1H), 3.19 (dd, $J = 5.5, 10.7$ Hz, 1H), 2.73 (dt, $J = 3.4, 13.6$ Hz, 1H), 2.31 (s, 1H), 2.26–1.98 (m, 8H), 1.93–1.82 (m, 7H), 1.72–1.19 (m, 5H), 1.55 (s, 3H), 1.38 (s, 3H), 1.12 (s, 3H), 1.10 (s, 3H), 0.97 (s, 3H), 0.91 (s, 3H), 0.77 (s, 3H); ^{13}C NMR (100 MHz, CDCl_3 , 300 K) δ 200.3, 172.5, 168.2, 152.0, 140.8, 135.2, 129.5, 129.2, 121.1, 78.9, 62.0, 55.1, 48.0, 45.6, 44.4, 43.3, 41.4, 39.3, 39.3, 37.5, 37.3, 33.0, 32.2, 31.5, 28.4, 28.3, 28.0, 26.6, 23.6, 18.9, 17.7, 16.6, 15.8; HREIMS m/z 589.3666 $[\text{M} + \text{H}]^+$ (calcd for $\text{C}_{35}\text{H}_{48}\text{N}_4\text{O}_4$, 588.3670).

Synthesis of Resin-Linked Glycyrrhetic Amide (2c). Amine-terminated Affi-Gel 10 (1 mL) **21** prepared by reduction of azide-terminal Affi-Gel **20** was treated with **19** (5 mL, 5 mg/mL) in CH_3CN for 12 h at 4 $^\circ\text{C}$. The resin was then washed with CH_3CN (3 \times 25 mL). The loading of **2c** was determined to be 2.2 ± 0.3 mg/mL by comparing the absorption at 254 nm (A_{254}) against standardized solutions of **1**.

(2S,4aS,6aS,6bR,10S,12aS,14bS)-N-(2-Azidoethyl)-10-hydroxy-2,4a,6a,6b,9,9,12a-heptamethyl-13-oxo-1,2,3,4,4a,5,6,6a,6b,7,8,8a,9,10,11,12,12a,12b,13,14b-icosahydricene-2-carboxamide (2d). HATU (189.7 mg, 0.50 mmol) was added to a mixture of glycyrrhetic acid (**1**) (78.3 mg, 0.17 mmol), 2-azidoethylamine (134.2 mg, 0.33 mmol), and Et_3N (142 μL , 0.83 mmol) in anhydrous DMF (1.2 mL). The reaction was stirred until the reaction contents dissolved, approximately 12 h at rt. The contents were evaporated under reduced pressure. The desired product **2d** (49.6 mg, 66%) was obtained after purification by flash chromatography (2:1 hexanes/EtOAc to 3:1 EtOAc/MeOH) as a white solid: R_f (0.13, 1:1 hexanes/EtOAc); ^1H NMR (400 MHz, CDCl_3 , 300 K) δ 5.96 (bs, 1H), 5.56 (s, 1H), 3.46 (s, 1H), 3.44 (m, 4H), 3.20 (dd, $J = 5.3, 10.8$ Hz, 1H), 2.77 (m, 1H), 2.28 (s, 1H), 2.31 (s, 1H), 2.14 (m, 1H), 2.02 (dt, $J = 4.5, 13.6$ Hz, 1H), 1.91 (m, 1H), 1.85–1.69 (m, 3H), 1.61 (m, 3H), 1.44–1.34 (m, 6H), 1.35 (s, 3H), 1.12 (s, 3H), 1.11 (s, 3H), 1.10 (s, 3H), 0.98 (s, 3H), 0.80 (s, 3H), 0.78 (s, 3H); ^{13}C NMR (100 MHz, CDCl_3 , 300 K) δ 200.4, 176.4, 169.4, 128.7, 79.0, 62.0, 55.1, 51.3, 51.1, 48.3, 45.6, 43.9, 43.4, 41.9, 39.4, 39.3, 37.6, 37.3, 32.9, 29.7, 28.7, 28.3, 27.5, 26.7, 26.6, 23.6, 18.9, 17.7, 16.6, 15.8; HRESIMS m/z 539.3884 $[\text{M} + \text{H}]^+$ (calcd for $\text{C}_{32}\text{H}_{50}\text{N}_4\text{O}_3$, 538.3883).

Acknowledgment. We thank S. Anderson (University of Texas Southwestern Medical Center) for assisting with the hybridoma experiments, Dr. A. Mercer for providing guidance in the use of the two-step Huisgen cycloaddition approach, Dr. Q. Li (the Center for Functional Genomics at the University of Albany) for protein ID analyses, Drs. X. Huang (UC San Diego) and A. Mrse (UC San Diego) for assistance with NMR analyses, Dr. Y. Su (UC San Diego) for mass spectral analyses, and Prof. E. Theodorakis (UC San Diego), Prof. V. Malhotra (UC San Diego), and Dr. A. Andres (UC San Diego) for helpful discussions.

Supporting Information Available: ^1H NMR, ^{13}C NMR, and selected 2D NMR spectra of the probes and intermediates are available free of charge via the Internet at <http://pubs.acs.org>.

References and Notes

- (1) (a) Koehn, F. E.; Carter, G. T. *Nat. Rev. Drug Discovery* **2005**, *4*, 206–220. (b) Kingston, D. G.; Newman, D. J. *Curr. Opin. Drug Discov. Dev.* **2005**, *8*, 207–227. (c) Overington, J. P.; AL-Lazikani, B.; Hopkins, A. L. *Nat. Rev. Drug Discovery* **2006**, *5*, 993–996. (d) Sams-Dodd, F. *Drug Discovery Today* **2005**, *10*, 139–147.
- (2) (a) Terstappen, G. C.; Schlüpen, C.; Raggiaschi, R.; Gaviraghi, G. *Nat. Rev. Drug Discovery* **2007**, *6*, 891–903. (b) Guiffant, D.; Tribouillard, D.; Gug, F.; Galons, H.; Meijer, L.; Blondel, M.; Bach, S. *Biotechnol. J.* **2007**, *2*, 68–75. (c) Markham, K.; Bai, Y.; Schmitt-Ulms, G. *Anal. Bioanal. Chem.* **2007**, *389*, 461–473.
- (3) Moses, J. E.; Moorhouse, A. D. *Chem. Soc. Rev.* **2007**, *36*, 1249–1262.
- (4) Peddibhotla, S.; Dang, Y.; Liu, J. O.; Romo, D. *J. Am. Chem. Soc.* **2007**, *129*, 12222–12223.
- (5) Smith, A. B.; Rucker, P. V.; Brouard, I.; Freeze, B. S.; Xia, S.; Horwitz, S. B. *Org. Lett.* **2005**, *7*, 5199–5202.
- (6) Alexander, M. D.; Burkart, M. D.; Leonard, M. S.; Portonovo, P.; Liang, B.; Ding, X.; Joullié, M. M.; Gullede, B. M.; Aggen, J. B.; Chamberlin, A. R.; Sandler, J.; Fenical, W.; Cui, J.; Gharpure, S. J.; Polosukhin, A.; Zhang, H. R.; Evans, P. A.; Richardson, A. D.; Harper, M. K.; Ireland, C. M.; Vong, B. G.; Brady, T. P.; Theodorakis, E. A.; La Clair, J. J. *ChemBioChem.* **2006**, *7*, 409–416.
- (7) Leslie, B. J.; Hergenrother, P. J. *Chem. Soc. Rev.* **2008**, *37*, 1347–1360.
- (8) (a) *Altern. Med. Rev.* **2005**, *10*, 230–237. (b) Asl, M. N.; Hosseinzadeh, H. *Phytother. Res.* **2008**, *22*, 709–724.
- (9) Hibasami, H.; Iwase, H.; Yoshioka, K.; Takahashi, H. *Int. J. Mol. Med.* **2006**, *17*, 215–219.
- (10) Laitinen, O. H.; Nordlund, H. R.; Hytonen, V. P.; Kulomaa, M. S. *Trends Biotechnol.* **2007**, *25*, 269–277.
- (11) Tao, L.; English, A. M. *Biochemistry* **2004**, *43*, 4028–4038.
- (12) Chida, K.; Sagara, H.; Suzuki, Y.; Murakami, A.; Osada, S.; Ohno, S.; Hirose, K.; Kuroki, T. *Mol. Cell. Biol.* **1994**, *14*, 3782–3790.
- (13) O'Brian, C. A.; Ward, N. E.; Vogel, V. G. *Cancer Lett.* **1990**, *49*, 9–12.
- (14) Martin, B. R.; Cravatt, B. F. *Nat. Methods* **2009**, *6*, 135–138.
- (15) Hughes, C. C.; MacMillan, J. B.; Gaudêncio, S. P.; Fenical, W.; La Clair, J. J. *Angew. Chem., Int. Ed.* **2009**, *48*, 728–732.
- (16) Liu, Y.; Shreder, K. R.; Gai, W.; Corral, S.; Ferris, D. K.; Rosenblum, J. S. *Chem. Biol.* **2005**, *12*, 99–107.
- (17) Yee, M. C.; Fas, S. C.; Stohlmeyer, M. M.; Wandless, T. J.; Cimprich, K. A. *J. Biol. Chem.* **2005**, *280*, 29053–29059.
- (18) Drahl, C.; Cravatt, B. F.; Sorensen, E. J. *Angew. Chem., Int. Ed.* **2005**, *44*, 5788–5809.
- (19) Evans, M. J.; Saghatelian, A.; Sorensen, E. J.; Cravatt, B. F. *Nat. Biotechnol.* **2005**, *23*, 1303–1307.
- (20) Adam, G. C.; Sorensen, E. J.; Cravatt, B. F. *Mol. Cell. Proteomics* **2002**, *1*, 781–790.
- (21) Low, W. K.; Dang, Y.; Schneider-Poetsch, T.; Shi, Z.; Choi, N. S.; Rzas, R. M.; Shea, H. A.; Li, S.; Park, K.; Ma, G.; Romo, D.; Liu, J. O. *Methods Enzymol.* **2007**, *431*, 303–324.
- (22) Wulff, J. E.; Siegrist, R.; Myers, A. G. *J. Am. Chem. Soc.* **2007**, *129*, 14444–14451.
- (23) Ulanovskaya, O. A.; Janjic, J.; Suzuki, M.; Sabharwal, S. S.; Schumacker, P. T.; Kron, S. J.; Kozmin, S. A. *Nat. Chem. Biol.* **2008**, *4*, 418–424.
- (24) Rizvi, S. A.; Courson, D. S.; Keller, V. A.; Rock, R. S.; Kozmin, S. A. *Proc. Natl. Acad. Sci. U. S. A.* **2008**, *105*, 4088–4092.
- (25) (a) Andersson, S.; Jornvall, H. *J. Biol. Chem.* **1986**, *261*, 16932–16936. (b) Lindqvist, A.; Andersson, S. J. *J. Biol. Chem.* **2002**, *277*, 23942–23948.

NP100371K